IEEE Transactions on Nuclear Science, Vol. NS-26, No. 3, June 1979

DISTRIBUTED SPUTTER-ION PUMPS FOR USE IN LOW MAGNETIC FIELDS

Jean-Michel Laurent and Oswald Gröbner*

1. Introduction

In electron storage rings a common solution for meeting the pump requirements in the long and hence conductance limited vacuum chambers, has been to install linear ion pumps in the field of the bending magnets[1]. These pumps form an integral part of the vacuum chamber and extend over that part of the machine circumference which is subjected to the desorbing action of the synchrotron light. For the vacuum system of LEP, integrated ion pumps have also been proposed[2]. However, a particular problem is that these pumps must operate at exceptionally low magnetic field levels-at injection typically 0.02 Tesla.

We have investigated firstly the dependence of the minimum field at which a pump cell of given size remains ignited as a function of the pressure and the anode voltage, taking as a measure of the pump performance the discharge intensity I/P i.e. the ratio of pump current and pressure. Secondly, using a calibrated test dome, the pumping speeds of various pump models were measured as function of the pressure, of the anode voltage and of the applied magnetic field. The ignition characteristics of pump cells with diameters ranging from 34 mm to 60 mm were studied. The integrated pumps have been designed for optimum conductance from the beam pipe to the active pumping volume. For this reason, we have constructed anode cylinders with perforated walls or anode structures consisting of 3 or 5 metal strips stacked in sandwich fashion with matching holes defining the anode cylinder.

2. Pump models

Because the total length of linear pumps in LEP amounts to about 20 km, a complex mechanical pump structure has to be avoided and we attach great importance to a design which is easy to produce in large quantities and reliable in operation. These considerations have determined the choice of diode pumps. A diode pump is also preferred because of its compact construction and because it uses more efficiently the limited space in the gap of the bending magnets.

The test pumps were designed to fit into an existing magnet 0.4 m long, with an aperture of 0.26 by 0.2 m. The pump cathodes were made of pure titanium plates and spaced by 7 cm. The height of the anode, made of stainless steel, has been 4 or 5 cm depending on the pump model. Since the magnet aperture was sufficiently wide, three rows of anode cells were combined into one anode structure of 27 to 30 cells in total. A variety of different cell sizes from 34 mm diameter up to 60 mm as well as various anode structures have been tested. As shown in Fig. 1, model C consists of cylindrical cells made of thin-walled tubes. For one of the pumps, type G, perforated anode cylinders have been used with the aim of increasing the conductance between the beam pipe and the active pumping volume.

The anodes of type P pumps have been assembled from several layers of thin perforated steel plates stacked with a spacing of several millimeters. The holes have been obtained by a photographic etching method analogous to the production of printed circuit boards. The diameter of the holes corresponds to the anode diameter - a complete stack being electrically equivalent to a conventional anode cylinder. Two versions of such sandwich type anodes with different hole sizes have been tested, version 3P, consisting of three layers and with 40 mm holes, and version 5P with five layers and 40 to 60 mm holes.

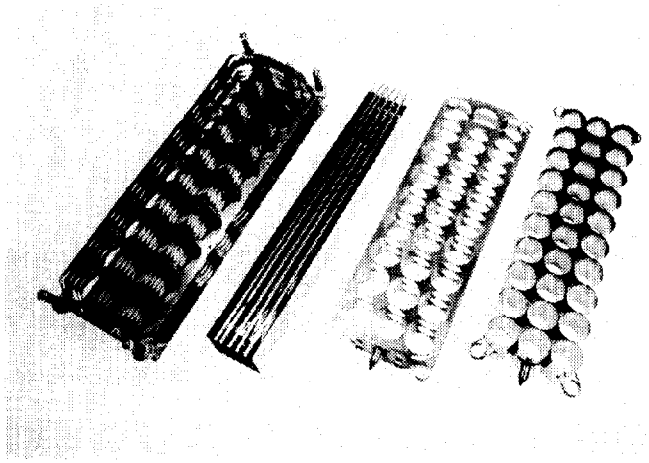

Fig. 1 Anode configurations used for pump tests : from left, anode assembled from 5 layers with 40 mm perforations (5P40); linear pump with single row of 50 mm holes and Ti-cathodes; anode with 3 layers and 40 mm holes (3P40), conventional cylinder anode with 36 mm diameter cells (C36).

3. Test apparatus

The pump elements were measured using a pumping speed test dome[3] fitted with a diaphragm of known conductance C. The pressure difference yields the pumping speed S through the relation $S = C \Delta p/p$. The test pump assembly is mounted in a separate vacuum chamber attached to the measuring dome and mounted in the dipole magnet. The magnet can be powered to any field value up to 0.22 T; it can be ramped to simulate the acceleration cycle in LEP. During the preparation of the system, which consists essentially of a bakeout at 300°C for 24 hours, the vacuum system is pumped successively by a mechanical pump group, a turbomolecular pump and a 60 ℓ/s sputter-ion pump. These pumps are valved off during pumping speed measurements. After a bakeout, the total pressure with the 60 ℓ/s sputter ion pump is typically in the low 10^{-10} torr range. The test pump is powered from a DC regulated high voltage supply adjustable between zero and 10 kV. Pump currents can be measured from about 10^{-9} A to 10 mA, the lower limit being determined by the leakage current of the insulators. After replacing the initially used ceramic feedthrough insulator by glass the leakage currents could be reduced to well below 10^{-8} A at 6 kV.

4. Discharge characteristic at low magnetic field

Several authors have studied the Penning discharge at low pressure and have proposed design concepts for diode ion pumps operating in high magnetic fields[4,5]. We have based our study on the work of W. Schuurman[6,7]. Assuming long Penning cells and a crossed field mobility of the electrons, proportional to ν_t/B^2, where ν_t is the total collision frequency and B the applied magnetic field, he derives expressions for the discharge intensity I/P, for the ignition field, B_i, and for the transition field B_t to the high magnetic field mode where the discharge intensity reaches a maximum. At injection the

*CERN, Geneva, Switzerland.

0018-9499/79/0600-3997$00.75 © 1979 IEEE

integrated pumps in LEP will operate close to the ignition field in the low magnetic field mode. Schuurman's result for the discharge intensity in a cell of radius r and length ℓ can be put in the form

$$I/P = \ell\left[a\left(\frac{\nu_i}{\nu_t}\right)^2 B^2r^2 - bv\right] \qquad (1)$$

where a and b are constants, ν_i/ν_t is the ratio of ionisation frequency and of the total collision frequency and v is the electron velocity corresponding to the ionisation potential of the gas molecules. The discharge ignites for $B_i r = \frac{8}{3}\frac{m}{e}\frac{\nu_c}{\nu_i}v$. Approximately[4], $rB_i = 3\ 10^{-4}$ Tm. However, we observe significant variations of this product with different anode structures, with pressure, see Fig. 2, and with anode voltage, Fig. 3. The pressure dependence of $B_i r$ in Fig. 2 can be fitted by the relation $B_i r = 2\ 10^{-4} - 3.5\ 10^{-5} \log_{10} p$. Furthermore, our results obtained with the sandwich type anode of 40 to 60 mm diameter support at constant p a scaling $r^n B_i$ = const., with n = 0.53. A particularly low starting field can be observed with the sandwich type pumps, 3P and 5P. Here the electron orbits appear not to be limited to the anode diameter resulting in an effective cell radius which is larger than for a cylinder anode. Some of our observations would indeed suggest that at very low fields the discharge does not remain confined to individual cells but rather fills uniformly the whole anode volume. The optimum anode voltage to ignite the discharge at low field has been found to be between 2 and 3 kV.

At transition to the high magnetic field mode the discharge intensity reaches a maximum . The transition field depends on the anode voltage U and is related to the ignition field through $B^2_t = 2(U/v)B_i/r$. Hence lowering the ignition field by increasing r, also lowers B_t and the maximum discharge intensity. Within limits this loss can be compensated by increasing U.

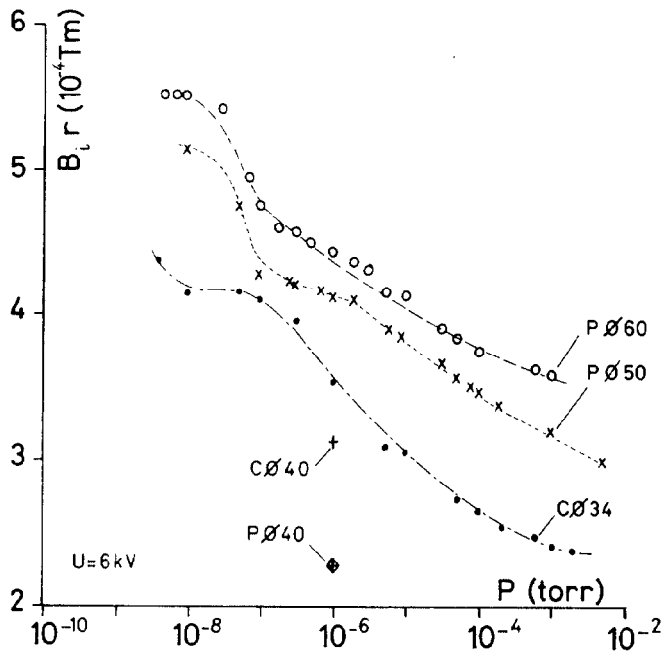

Fig. 2 $B_i r$ versus nitrogen pressure for various anode configurations with 6 kV anode voltage.

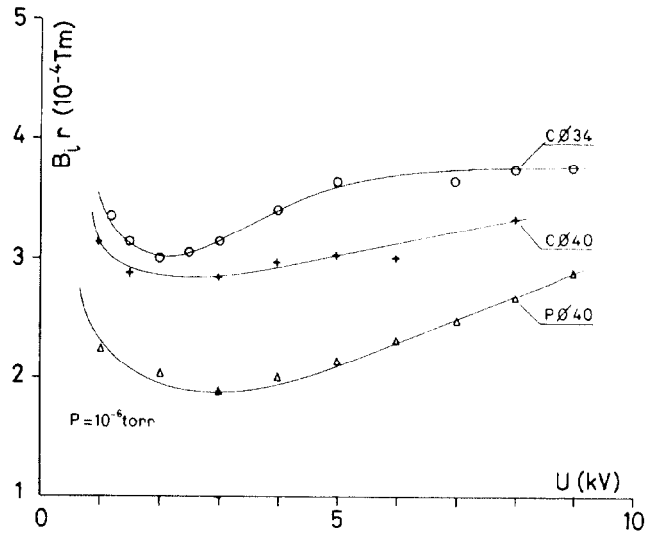

Fig. 3 $B_i r$ versus anode voltage for different anode configurations and 10^{-6} torr nitrogen pressure

5. Results of pumping speed measurements

The dependence of the pumping speed on the magnetic field, voltage, cell diameter, anode structure, bakeout temperature and on operating conditions have been studied. The pumping speed S as function of the magnetic field is shown in Fig. 4.

All curves exhibit an approximately linear rise of S at low magnetic field followed by a maximum at the transition to the high magnetic field mode[8]. The highest pumping speed has been observed with the pump model 5P. We attribute the low speed of the model 3P to the fact that the anode is not sufficiently closed to confine the discharge.

The existence of an optimum anode voltage for a given magnetic field is illustrated in Fig. 5. The requirement of a low anode voltage for igniting the

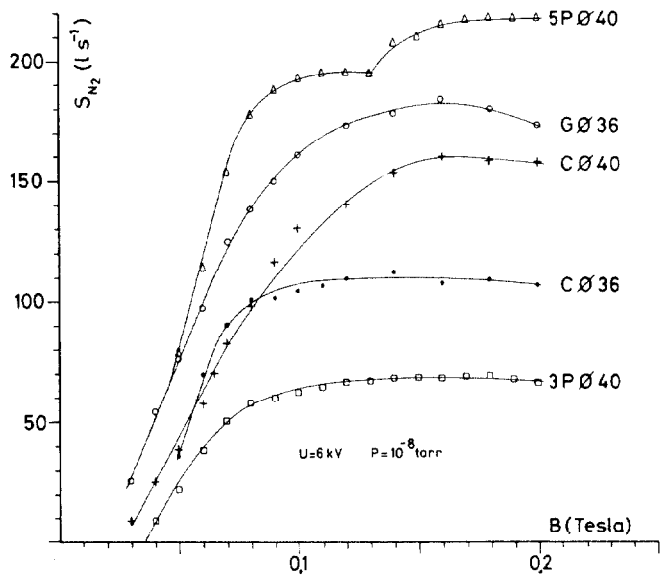

Fig. 4 Pumping speed for nitrogen versus magnetic field for various anodes including a perforated cylinder anode of 36 mm diameter (type G).

discharge at low magnetic field and of a high voltage to increase B_t and hence the pumping speed at high field, leads to a pump voltage increasing proportional with the magnetic field. For the linear pumps of LEP, optimum performance would imply an increase of the anode voltage from about 2 kV at the injection field to 6 kV at the full field. The conditioning of the pump, in particular the bakeout temperature has a significant effect on the pumping speed, as shown in Fig. 6. Following a 200°C bakeout, which can be considered acceptable for an aluminium vacuum chamber, the effective pumping speed is only 80% of the value for a 300°C bakeout; this is reduced to 50% for a bakeout at 150°C. We have observed a similar important reduction in pumping speed for a pump operating above ambient temperature. In fact, after a 300°C bakeout, only 60% of the initial speed remains when the temperature of the pump is increased to 100°C. For the integrated pumps in LEP, which are exposed to large amounts of scattered synchrotron radiation, this effect may become important unless adequate cooling of the pump elements is provided.

Between the different pump models we have observed large variations of the ratio between measured values of pumping speed and discharge intensity. Typical results for 34 mm cylinder cells and for 40 mm sandwich type anode cells are presented in Fig. 7. Our results obtained with cylinder cells are in good agreement with the average values of 0.075 quoted for diode sputter ion pumps[8]. However, for the same operating conditions the pump elements 5P yield about twice this value. The large discharge intensity of this anode structure provides a more than proportionally higher pumping speed than the cylinder type anode (see Fig. 4).

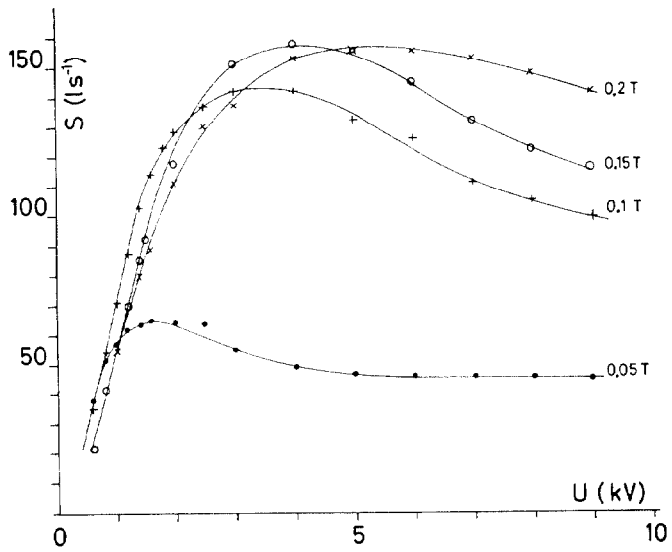

Fig. 5 Pumping speed for nitrogen versus anode voltage for different magnetic fields. Measured with an anode of 27 cylinders of 40 mm diameter and 50 mm length (type C40).

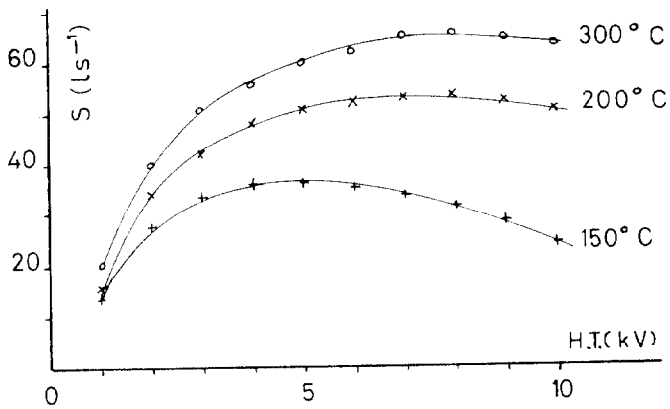

Fig. 6 Pumping speed for nitrogen as function of anode voltage for different bakeout temperatures measured with a 5P50 type anode at 0.1 T.

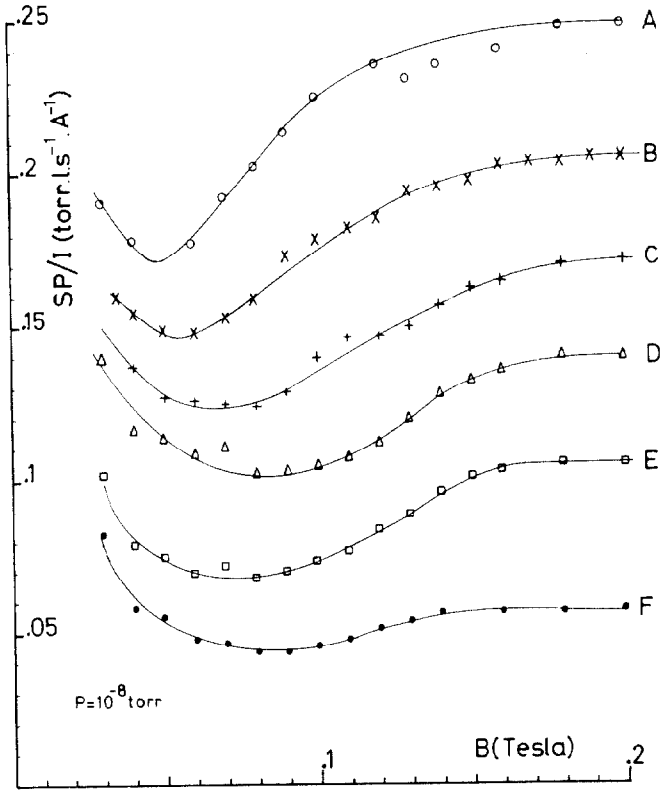

Fig. 7 Ratio of pressure to discharge intensity (SP/I) versus magnetic field at 10^{-8} torr nitrogen for a 5P40 type anode, curves A,B,C and a C34 type anode, curves D,E,F. Curves A,B,C show the effect of the anode voltage, respectively 4,6 and 8 kV, after a 300°C bakeout. Curves D,E,F show the effect of the bakeout temperature, 300°C, 200°C and 150°C.

Summary

Measurements of the ignition characteristic of large diameter anode cells indicate a more than proportional increase of cell radius for a given reduction of B_i. Considerations of conductance have lead to an open anode configuration with several layers of perforated metal sheets. The pumping speed is found to be larger than for anodes with conventional cylinders. Moreover, since the electrons can move more freely inside the anode the discharge ignites at a lower magnetic field. Scaling from our measurements on model pumps, we expect to obtain with a single row of anode cells, designed to ignite at a field below 0.02 T, a linear pumping speed of about 60 ℓ/sm at a transition field of about 0.1 T.

References

[1]CSR, PEP, PETRA, SPEAR, VEPP-2, VEPP-4.
[2]The LEP Study Group, CERN Internal Report, CERN-ISR-LEP/78-17, (1978).
[3]E. Fischer, H. Mommsen, CERN-ISR/VAC/66-11 (1966).
[4]M.D. Malev, Vacuum, Vol. 23, 11 (1973).
[5]R.L. Jepsen, J. Appl. Phys. Vol. 32, no. 12, (1961).
[6]W. Schuurman, Physica 36, 136 (1967).
[7]W. Schuurman, Physica 43, pp. 513-516 (1969).
[8]H. Hartwig, J.S. Kouptsidis, J. Vac. Sci. Technol., Vol. 11, 6 (1974).